*instruments*

MDPI

*Article*

# Tracker-in-Calorimeter (TIC) Project: A Calorimetric New Solution for Space Experiments †

**Gabriele Bigongiari [1,2,*], Oscar Adriani [3,4], Giovanni Ambrosi [5], Philipp Azzarello [6], Andrea Basti [1], Eugenio Berti [3,4], Bruna Bertucci [5,7], Lorenzo Bonechi [4], Massimo Bongi [3,4], Sergio Bottai [4], Mirko Brianzi [4], Paolo Brogi [1,2], Guido Castellini [4,8], Enrico Catanzani [5,7], Caterina Checchia [1,2], Raffaello D'Alessandro [3,4], Sebastiano Detti [4], Matteo Duranti [5], Noemi Finetti [4,9], Valerio Formato [10], Maria Ionica [5], Paolo Maestro [1,2], Fernando Maletta [4], Pier Simone Marrocchesi [1,2], Nicola Mori [4], Lorenzo Pacini [4,8], Paolo Papini [4], Sergio Bruno Ricciarini [4,8], Gianluigi Silvestre [5,7], Piero Spillantini [4], Oleksandr Starodubtsev [4], Francesco Stolzi [1,2], Jung Eun Suh [1,2], Arta Sulaj [1,2], Alessio Tiberio [3,4] and Elena Vannuccini [4]**

1 INFN Pisa, Largo Bruno Pontecorvo 3, I-56127 Pisa, Italy
2 Dipartimento di Scienze Fisiche, Della Terra e dell'Ambiente, Università di Siena, Strada Laterina 8, I-53100 Siena, Italy
3 Dipartimento di Fisica e Astronomia, Università di Firenze, Via G. Sansone 1, Sesto Fiorentino, I-50019 Firenze, Italy
4 INFN Firenze, Via B. Rossi 1, Sesto Fiorentino, I-50019 Firenze, Italy
5 INFN Perugia, Via A. Pascoli, I-06100 Perugia, Italy
6 Département de Physique Nucléaire et Corpusculaire, University of Geneva, CH-1211 Geneva, Switzerland
7 Dipartimento di Fisica e Geologia, Università di Perugia, Via A. Pascoli, I-06100 Perugia, Italy
8 IFAC (CNR), Via Madonna del Piano 10, Sesto Fiorentino, I-50019 Firenze, Italy
9 Dipartimento di Scienze Fisiche e Chimiche, Università dell'Aquila, Via Vetoio, Coppito, I-67100 L'Aquila, Italy
10 INFN Roma Tor Vergata, I-00133 Rome, Italy
* Correspondence: gabriele.bigongiari@pi.infn.it; Tel.: +39-050-2214-349
† This paper is based on the talk at the 19th International Conference on Calorimetry in Particle Physics (CALOR 2022), University of Sussex, Brighton, UK, 16–20 May 2022.

check for updates

**Citation:** Bigongiari, G.; Adriani, O.; Ambrosi, G.; Azzarello, P.; Basti, A.; Berti, E.; Bertucci, B.; Bonechi, L.; Bongi, M.; Bottai, S.; et al. Tracker-in-Calorimeter (TIC) Project: A Calorimetric New Solution for Space Experiments. *Instruments* **2022**, *6*, 52. https://doi.org/10.3390/instruments6040052

Academic Editors: Fabrizio Salvatore, Alessandro Cerri, Antonella De Santo and Iacopo Vivarelli

Received: 30 August 2022
Accepted: 20 September 2022
Published: 26 September 2022



**Abstract:** A space-based detector dedicated to measurements of $\gamma$-rays and charged particles has to achieve a balance between different instrumental requirements. A good angular resolution is necessary for the $\gamma$-rays, whereas an excellent geometric factor is needed for the charged particles. The tracking reference technique of $\gamma$-ray physics is based on a pair-conversion telescope made of passive material (e.g., tungsten) coupled with sensitive layers (e.g., silicon microstrip). However, this kind of detector has a limited acceptance because of the large lever arm between the active layers, needed to improve the track reconstruction capability. Moreover, the passive material can induce fragmentation of nuclei, thus worsening charge reconstruction performances. The Tracker-In-Calorimeter (TIC) project aims to solve all these drawbacks. In the TIC proposal, the silicon sensors are moved inside a highly-segmented isotropic calorimeter with a couple of external scintillators dedicated to charge reconstruction. In principle, this configuration has a good geometrical factor, and the angle of the $\gamma$-rays can be precisely reconstructed from the lateral profile of the electromagnetic shower sampled, at different depths in the calorimeter, by silicon strips. The effectiveness of this approach has been studied with Monte Carlo simulations and validated with beam test data of a small prototype.

**Keywords:** cosmic rays; astroparticles; $\gamma$-ray astronomy

## 1. Introduction

A calorimeter coupled to a charge detector is the typical instrument configuration for direct measurement experiments of the Cosmic Ray (CR) elemental spectra. This setup can easily be scaled to cover the desired energy range of the high-energy cosmic radiation. Recently, the ongoing CALET [1] and DAMPE [2,3] experiments, based on this concept,

reported results on the H and He spectra over a wide energy range and revealed interesting spectral characteristics. However, current missions are limited by the acceptance, which prevents them from going beyond 100 TeV due to the decreasing flux at higher energies. In fact, to scan the "knee" regions of the individual H, He, and Nuclei spectra, an acceptance of at least 2.5 $m^2sr \times 5$ years and an energy resolution better than 40% are needed. On the other hand, calorimetric CR measurements conducted in space also have the ability to study the inclusive electronic component (e.g., CALET and DAMPE experiments were specifically designed to study the high-energy electron+positron spectrum). To improve the quality of the electron + positron flux measurements, the electromagnetic showers must have an energy resolution of at least 2% and an electron/hadron rejection power greater than $10^6$, as well as an acceptance larger than the hadron acceptance (of at least 3.6 $m^2sr \times 5$ years). All these requirements place further constraints on the instrument. A full treatment of problems connected to the design and construction of an apparatus for high-energy cosmic rays can be found in [4], containing an extensive description of the future High-Energy cosmic-Radiation Detection (HERD) facility; the requirements and the expectations of such kinds of experiments are described as well.

Moreover, in a modern multi-messenger space experiment, $\gamma$-rays detection also plays an important role. A good angular resolution, which allows for the precise identification of astrophysical sources, is a fundamental requirement for $\gamma$-ray astronomy. The direction of the incoming photon can be reconstructed by a pair-conversion telescope. A pair-conversion instrument detects high-energy $\gamma$-rays by exploiting a passive material, generally thin foils of dense metal, commonly tungsten, in which electron–positron pairs are generated and then using standard particle-physics techniques, such as a silicon microstrip detectors, to detect these particles. This kind of detector is the standard tracker used for $\gamma$-ray physics in the energy region above 100 MeV, and it has been installed in recent experiments, such as Fermi [5] and AGILE [6] (see Figure 1 left panel). The minimum specifications for the Large-Area Telescope of Fermi experiment, in the energy range 20 MeV–300 GeV, are an angular resolution less than 0.15° above 10 GeV (less than 3.5° above 100 MeV) with an energy resolution better than 10% and a field of view larger than 2 sr. Such a geometry suffers some disadvantages. First of all, the acceptance is limited by the large lever arm between the active sensors needed to improve the tracking performance. In addition, the presence of dense passive material reduces the mass budget available for the calorimeter. Moreover, tungsten layers can induce fragmentation of nuclei, thus worsening the charge reconstruction performance of the apparatus. The main purpose of the Tracker-In-Calorimeter (TIC) project, approved and financed by INFN (Italy) in 2017, is the development of a detector with good angular resolution, needed for $\gamma$-rays, and a good geometric factor, needed for charged particles. This work summarizes the results of the TIC collaboration, extensively described in [7].

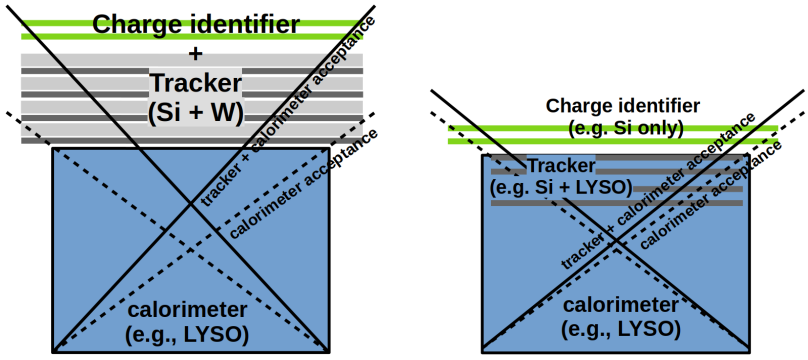


**Figure 1.** Conceptual designs of the two different detector geometries for $\gamma$-ray physics: on the **left**, the standard approach with a external tracker on the top of a calorimeter, and on the **right**, the TIC approach with a silicon tracker integrated inside a calorimeter.

## 2. Problems and Proposed Solution

The major constraint in achieving the above-mentioned performance is the weight limitation for these types of detectors (a few tons), which has a significant impact on both geometrical factors and energy resolution. A starting point for a possible solution could be the proposal for a homogeneous and isotropic calorimeter made by the CaloCube collaboration [8]. The CaloCube concept design was adopted by the future HERD experiment [4], which was proposed as one of several space astronomy payloads aboard the future Chinese Space Station. The suggested solution is a big cube composed of cubic scintillating crystals read out by photodiodes (PDs) (see Figure 2). The "Rubik" geometry and homogeneity allow particles to be collected from either the top or lateral faces, optimizing geometrical acceptance for a fixed mass budget. The active absorber gives good energy resolution, and the high granularity enables shower imaging, which provides criteria for both leakage correction and electron/hadron separation.

The CaloCube architecture was tuned for the detection of nuclei in the TeV–PeV energy region. A total weight of 2 tons, including both active and passive materials, was assumed. A comparative study of different scintillating materials with a wide variety of densities and calorimetric and optical characteristics was carried out. The results favor materials with superior shower confinement (e.g., Lutetium Yttrium Orthosilicate, LYSO), which compensate for the reduced volume due to these crystals' higher density and shorter interaction length. An effective geometric factor of up to 4 $m^2$sr can be obtained, with an energy resolution greater than 40%. The projected performance for electrons and $\gamma$-rays is a geometric factor of up to 3.4 $m^2$sr and an energy resolution greater than 2%. A detailed description of the Calocube project, the optimization of the detector design (also in terms of mass budget), and the results of beam tests of the prototype can be found in [9].

The TIC project aims to optimize a homogeneous calorimeter, such as CaloCube, to track $\gamma$-rays. A photon hitting the calorimeter starts an electromagnetic shower developing inside it. Such a segmented detector can sample the shower profile at different points. In principle, from this information, the shower axis can be reconstructed, and then the incoming direction and the impact point of the photon. Using a sampling calorimeter [10], it is possible to obtain a resolution better than 100 μm on the impact point of electrons above 100 GeV. The same results are expected for photons. In practice, in the TIC approach, the main tracker is removed and integrated inside a calorimeter, CaloCube-like, thus removing the problems previously described. The TIC conceptual design is shown in Figure 1 (right panel). In this scheme, one side of the calorimeter is instrumented with silicon microstrips (the sensitive layer of the tracker) interleaved with some layers of thin scintillating crystals (the $\gamma$-ray converter layers of the tracker). The proposed geometry is shown in Figure 3.

On the upper face, a stack of three layers of thin crystals interleaved by four silicon microstrip detectors has been added. A standard silicon sensor consists of an array of narrow strips (a few hundred um width, many cm long) aligned along a direction (X or Y), and it can sample the signals only along the perpendicular direction (Y or X). To measure both coordinates, coupling two sensors, with strips orthogonal to each other, is required. The gap (7 cm) between the first two silicon layers is necessary to mitigate the effect of the multiple scattering of the generated electron–positron pair on the tracking power. The key point is the fine sampling (hundreds of μm) of the initial part of the electromagnetic shower by the silicon strips (with respect to the crystals, a few cm thick) that allows increasing the tracking accuracy of the whole apparatus.

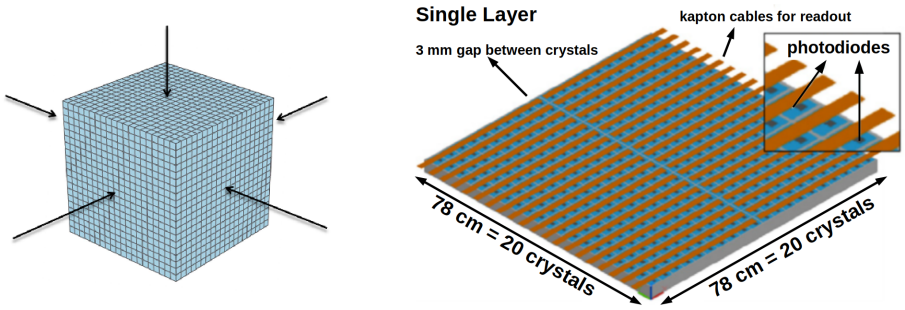


**Figure 2.** Conceptual design of the CaloCube 3D highly segmented calorimeter: on the **left**, the complete cubic detector; on the **right**, 1 of the 20 layers (from [8]).

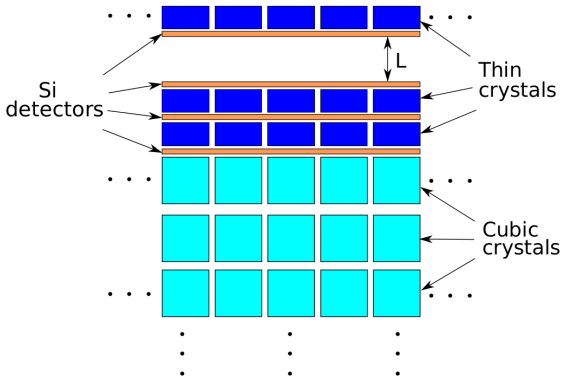


**Figure 3.** Schematic side view of the upper face of the simulated TIC: on the top, 3 scintillator layers made of thin crystals (blue) plus 4 silicon microstrip layers (orange) interleaved in; on the bottom, some layers made of cubic crystals (cyan) from CaloCube (from [7]).

## 3. Monte Carlo Simulations

A Monte Carlo simulation, based on the FLUKA package [11], has been set up in order to verify the validity of the proposal and quantify the performance of the detector. The simulated geometry derives from the design of the future HERD calorimeter [4], composed of cubic crystals, made up of LYSO (see Figure 3). The basic calorimeter is an ensemble of $21 \times 21 \times 21$ small cubic bricks, 3.5 cm thick, interleaved by 5 mm carbon fibers, simulating the support structure. The total depth is $\sim$3.2 interaction lengths ($\lambda_I$) and $\sim$58 radiation lengths ($X_0$). On the top of the designated upper face, the fine tracker, i.e., a stack of silicon microstrips and thin crystals, is installed. Monochromatic beams of $\gamma$-rays at different energies (1, 10, and 100 GeV), uniformly illuminating the entire upper face, with an isotropic angular distribution, have been simulated.

The track of a photon impinging the calorimeter can be reconstructed by applying a multi-step procedure to the crystal and Si-strip signals, described in the Section 4. The angular resolution obtained with the simulated data as a function of the $\gamma$-ray energy is shown in Figure 4, compared to those of Fermi and DAMPE. The performance of the tracking algorithm also depends on the efficiency of event selection used for the analysis. In Figure 4, the results of the analysis with two different selections are presented. A complete description of this analysis can be found in [7]. For Fermi and DAMPE efficiency calculations, see [12,13].

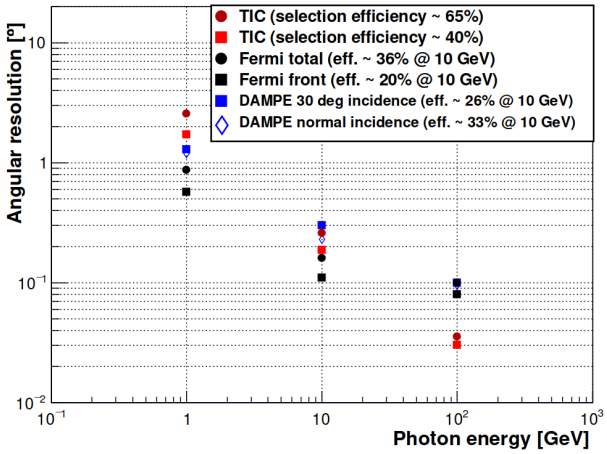


**Figure 4.** Angular resolution vs. Photon Energy: TIC compared to Fermi and DAMPE (from [7]).

The performance improves as energy increases for all the experiments. This behavior depends on two effects. At lower energies, the multiple scattering in the converting materials limits the tracking accuracy. The TIC crystals are thicker than the pair-conversion telescopes of FERMI and DAMPE, and this means a worse resolution. At higher energies, FERMI and DAMPE are constrained by the position resolution of their tracking systems, which then improves to an asymptote. Instead, in the TIC calorimeter, the statistical fluctuations of the electromagnetic shower decrease, leading to a more precise sampling of the signals and then improved tracking performance. At around 100 GeV, the resolution of TIC is better than that of FERMI and DAMPE.

## 4. Track Reconstruction Method

A particle (photon) traversing the detector releases energy in both crystals and silicon strips. Starting from this information (signals), it is possible in principle to reconstruct the particle track and then the original direction of the incoming particle. This is the goal of an apparatus dedicated to $\gamma$-rays physics. Therefore, the track reconstruction algorithm, used for the data analysis, is fundamental to verifying the potential of the detector design. A multi-step procedure has been developed based on the Principal Component Analysis method (PCA). The starting point is the selection, event by event, of the crystals with a signal above a given threshold (i.e., a few sigmas above the electronic noise). Let $\mathbf{N}$ be the number of the selected crystals. From the coordinates $\mathbf{c_i^{(n)}}$ (with i = X, Y, Z and n = 1, . . . , N) of these crystals, the corresponding covariance matrix $\mathbf{M_{ij}^{CAL}}$ can be calculated:

$$\mathbf{M_{ij}^{CAL}} = \frac{1}{\sum_{n=1}^{N} \mathbf{S_{CAL}^{(n)}}} \sum_{n=1}^{N} \mathbf{S_{CAL}^{(n)}} (\mathbf{c_i^{(n)}} - \mathbf{C_i})(\mathbf{c_j^{(n)}} - \mathbf{C_j}) \quad \text{where} \quad \mathbf{C_{i/j}} = \frac{\sum_{n=1}^{N} \mathbf{S_{CAL}^{(n)}} \mathbf{c_{i/j}^{(n)}}}{\sum_{n=1}^{N} \mathbf{S_{CAL}^{(n)}}}.$$

In these formulas, $\mathbf{C_{i/j}}$ (with i/j = X,Y,Z) is the center of gravity (c.o.g.) of the coordinates of the selected crystals, whereas $\mathbf{S_{CAL}^{(n)}}$ (with n from 1 to N) are the crystal signals, used as weights for both calculations (covariance matrix and c.o.g.). From the $\mathbf{M_{ij}^{CAL}}$ matrix, the eigenvectors can be extracted. The eigenvector with the largest eigenvalue represents a first estimation of the particle track, based on the calorimeter signals only.

The next step is to introduce the silicon detector. As explained before, a silicon strip sensor can measure only one transverse coordinate (X or Y in TIC geometry). So, the algorithm described below has to be repeated twice, for X–Z and Y–Z views. Let $\mathbf{J}$ be the strips in a view with a signal exceeding a threshold based on the system noise. From the

coordinates $\mathbf{d_i^{(k)}}$ (with i = X, Z or Y, Z and k = 1, . . . , J) of the selected strips, the covariance matrix $\mathbf{M_{ij}^{SIL}}$ is calculated by the formula:

$$\mathbf{M_{ij}^{SIL}} = \frac{1}{\sum_{k=1}^{J} \mathbf{W_{SIL}^{(k)}}} \sum_{k=1}^{J} \mathbf{W_{SIL}^{(k)}} (\mathbf{d_i^{(k)}} - \mathbf{D_i})(\mathbf{d_j^{(k)}} - \mathbf{D_j}) \quad \text{where} \quad \mathbf{D_{i/j}} = \frac{\sum_{k=1}^{J} \mathbf{W_{SIL}^{(k)}} \mathbf{d_{i/j}^{(k)}}}{\sum_{k=1}^{J} \mathbf{W_{SIL}^{(k)}}}.$$

This time, $\mathbf{D_{i/j}}$ (with i/j = X, Z or Y, Z) is the c.o.g. of the coordinates of the selected strips. The core of the whole algorithm is the definition of the weights $\mathbf{W_{SIL}^{(k)}}$ (with k = 1, . . . , J) used in the matrix calculation. A simple estimation can be the ratio between the signal $\mathbf{S^{(k)}}$ from the k-th strip and the total energy $\mathbf{S_P}$ measured by the plane containing the k-th strip. However, the impact point of the particle on each silicon plane can be estimated using the calorimeter track. The extrapolated transverse coordinate $\mathbf{X_P}$ of this point is distributed according to a Gaussian function. The combination of signal information and coordinate spatial dispersion has been found as the best estimation for the weighting factor of the k-th strip, according to the formula:

$$\mathbf{W_{SIL}^{(k)}} = \frac{\mathbf{S^{(k)}}}{\mathbf{S_P}} \cdot \frac{1}{\sqrt{2\pi}\sigma_P} \mathbf{exp}\left[-\frac{1}{2}\left(\frac{\mathbf{d_{X/Y}^{(k)}} - \mathbf{X_P}}{\sigma_P}\right)\right]$$

where $\sigma_P$ is the standard deviation of Gaussian dispersion, estimated by simulation. This definition connects the calorimeter and the silicon strip tracking. The eigenvector with the largest eigenvalue of the matrix $\mathbf{M_{ij}^{SIL}}$ represents a reconstructed track improved with respect to the previous one. Since the weights can be recalculated using the new estimate of the impact point from this new track, the whole procedure can be repeated until convergence. A detailed description of the algorithm can be found in [7].

## 5. Prototype and Beam Test Results

The simulation results have been further validated by building a small prototype. Its configuration is shown in Figure 5. The main part has been obtained from the refurbished CaloCube prototype [9]. In front of the calorimeter (represented by the horizontal blue modules in Figure 5), a module based on the TIC design has been added. This part was in turn composed of two sub-parts. The first one was made of two layers of thin crystals with, in the middle, two silicon layers separated by a gap, as in the schematic of Figure 3. The second one was a kind of "sandwich" made of alternate layers of silicon strips and crystals. The thin crystals of the first two layers were CaloCube spare cubes sawn in half. The silicon detectors were spare sensors from the DAMPE experiment [14]. The material, CsI(Tl), used for Calocube is different from the LYSO of the simulations of the full-scale detector. Then, a dedicated simulation has been developed.

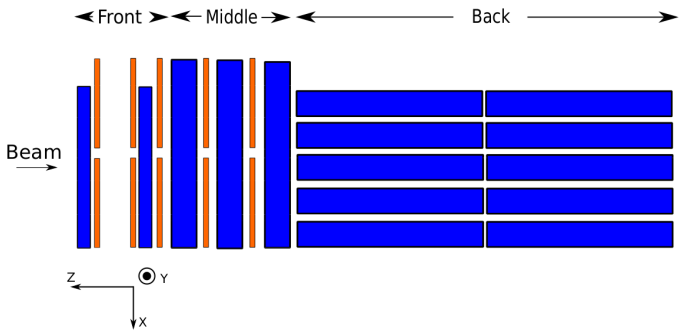


**Figure 5.** Top view of the TIC prototype: the blue modules represent the trays containing the crystals; the silicon sensors are in orange (from [7]).

The limited number of available silicon modules was sufficient only to instrument one view, and then the tracker was able to reconstruct only the XZ projection of the

particle trajectory. The prototype has been tested at the CERN accelerators with electron beams. The choice of electrons instead of photons has been made only for practical reasons. Nevertheless, since the tracking method is based on the sampling of electromagnetic showers, the performance of the detector with electrons is expected to be virtually identical to those with photons. In the beam test area, the support structure allowed the whole apparatus to move up and down and rotate and then modify the angle and the impact point of the particles. During the test, the energy of the beam was varied from 1 GeV to 100 GeV and the incidence angle from 0 to 10 degrees. The response calibration and the alignment of the instrument have been realized with a muon beam. The analysis of the beam test data is based on the same reconstruction procedure applied to simulations described in Section 4.

The algorithm reconstructs the tracks of particles impinging the detector. The dispersion of the reconstructed incoming directions around the true incidence angles is a good estimator of the TIC performance. The true incidence is unknown by definition, but it can be evaluated from the mean of the distribution of reconstructed angles with the detector in a fixed position. This evaluation is naturally affected by a bias that was considered in the simulation. The dedicated simulation, based on FLUKA, included an accurate description of the experimental environments. The particle generator has been set also to reproduce the real beam line, according to specifications provided by CERN. Moreover, some instrumental effects, such as the capacitive coupling of microstrips and the electronic noise, were taken into account as well.

In Figure 6. the distributions of dispersion around the mean angle, in the case of 1 GeV and 5 GeV electrons, are shown: the agreement between the real and simulated data is very good. In this energy region, below 50 GeV, the angular resolution is intrinsically worse, and the tuning of the simulation seems sufficient to correctly model the detector behavior. However, the accuracy of simulations becomes progressively more important at higher energies. Above 50 GeV, it is necessary to introduce an additional spread (of about 0.04°) to the nominal one of the simulated beam to obtain a quite good agreement with real data. The effect of this extra "fine-tuning" to accurately reproduce the real angular volatility is evident in Figure 7, showing the dispersion distributions of test beam data (black curve) in comparison with simulations (red and blue curves).

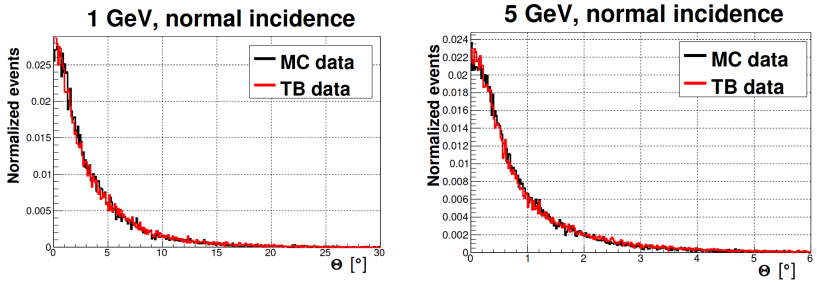


**Figure 6.** Angular resolution of the reconstructed tracks for 1 and 5 GeV electrons (from [7]).

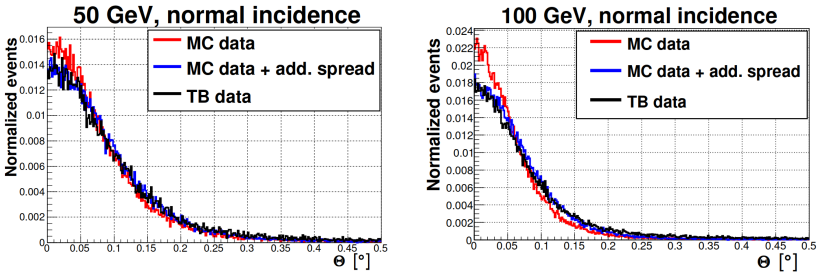


**Figure 7.** Angular resolution of the reconstructed tracks for 50 and 100 GeV electrons (from [7]).

This correction accounts for unknown systematic effects affecting the apparatus in the whole energy range. The residual test beam–Monte Carlo resolution difference gives an estimation of systematic error. A detailed description of Monte Carlo tuning and the

study of systematic errors can be found in [7]. The angular distributions of reconstructed photons are well described by a Point Spread Function (PSF). The width of these dispersion distributions measures the precision of the tracking performance of TIC at different energies. A description of the determination method of PSF for a $\gamma$-ray space experiment (FERMI) can be found in [15]. In Table 1, the results for 68% PSF containment radius are summarized: the agreement between simulated and real data is quite satisfactory.

**Table 1.** Summary of results: XZ angular resolution from test beam (TB) and Monte Carlo (MC) data for 68% PSF (derived from [7]).

| Energy (GeV) | Angle (Deg) | Res. 68% (Deg)—TB | Res. 68% (Deg)—MC |
|---|---|---|---|
| 1 | 0 | $3.72 \pm 0.11$ | $3.87 \pm 0.12$ |
| 5 | 0 | $0.985 \pm 0.016$ | $0.955 \pm 0.014$ |
| 10 | 0 | $0.4095 \pm 0.0087$ | $0.3971 \pm 0.0050$ |
| 50 | 0 | $0.1205 \pm 0.0023$ | $0.0995 \pm 0.0050$ |
| 100 | 0 | $0.0897 \pm 0.0010$ | $0.0680 \pm 0.0008$ |
| 100 | 10 | $0.0884 \pm 0.0013$ | $0.0646 \pm 0.0004$ |

Instead, the agreement at 95% PSF is not as good as it looks in Table 2. The worsening is probably due to residual instrumental effects not reproduced by Monte Carlo simulation. This results in a different shape of tails of the distributions. On the other hand, the effect on the angular resolution of the particle impact angle is negligible. In Tables 1 and 2 (last two lines), the results for 100 GeV electrons with $0^\circ$ and $10^\circ$ incidence angles are shown: the resolutions are perfectly compatible.

**Table 2.** Summary of results: XZ angular resolution from test beam (TB) and Monte Carlo (MC) data for 95% PSF (derived from [7]).

| Energy (GeV) | Angle (Deg) | Res. 95% (Deg)—TB | Res. 95% (Deg)—MC |
|---|---|---|---|
| 1 | 0 | $10.63 \pm 0.15$ | $11.44 \pm 0.33$ |
| 5 | 0 | $3.300 \pm 0.063$ | $3.282 \pm 0.054$ |
| 10 | 0 | $1.946 \pm 0.062$ | $1.790 \pm 0.068$ |
| 50 | 0 | $0.921 \pm 0.029$ | $0.710 \pm 0.058$ |
| 100 | 0 | $0.678 \pm 0.033$ | $0.308 \pm 0.010$ |
| 100 | 10 | $0.662 \pm 0.036$ | $0.259 \pm 0.019$ |

## 6. Conclusions

The TIC collaboration developed a new detector for Cosmic Ray experiments, starting from the experience of the CaloCube project, which developed a compact cubic calorimeter. This design maximizes instrument acceptance, respecting the limit on the mass budget of space-based missions. This is crucial to extend the energy measure of charged Cosmic Rays until the PeV region. The TIC idea was the integration of a silicon tracker inside this high-segmented calorimeter to optimize its design also for $\gamma$-rays physics: the installation of silicon microstrips permits the tracking accuracy needed for high-energy photons. Different geometries have been investigated using simulations: the expected performances are comparable with the main $\gamma$-ray experiments (Fermi, DAMPE). A small-scale prototype has been built and tested at CERN laboratories with electron beams. The analysis of the collected data confirmed the expectations in the energy range from 1 GeV to 100 GeV; above 50 GeV, the measured angular resolution is even better than Fermi and DAMPE. At 68% PSF, the test data are in good agreement with Monte Carlo studies. This validates the simulation predictions of the full-scale detector and provides a robust validation of the measurement principle. These promising results represent an important contribution to the development of new instruments for astroparticle experiments. The TIC design has been considered during the planning of the HERD mission mentioned above. In addition, the TIC geometry can be further improved. In the original scheme, the deep homogeneous calorimeter can

provide a very precise measure of photon energy, but the $\gamma$-ray acceptance is constrained by the fact that only one face of a cubic calorimeter is instrumented with silicon sensors. A possible development could be instrumenting the other faces and then extending the energy range beyond 300 GeV (the limit of the FERMI experiment). Interesting perspectives could open up in the coming years for $\gamma$-ray physics.

**Author Contributions:** Data curation, E.B., L.P. and E.V.; Formal analysis, S.B. and P.P.; Resources, S.D. and O.S.; Supervision, O.A., G.A., B.B., G.C., M.D., P.S.M., P.S. and R.D.; Visualization, A.B., L.B., M.B. (Massimo Bongi), M.B. (Mirko Brianzi), P.B., E.C., C.C., N.F., V.F., M.I., P.M., F.M., S.B.R., G.S., F.S., J.E.S., A.S., A.T. and P.A.; Writing—original draft, G.B.; Writing—review & editing, N.M. All authors have read and agreed to the published version of the manuscript.

**Funding:** This research received no external funding.

**Data Availability Statement:** Not applicable.

**Conflicts of Interest:** The authors declare no conflict of interest. The funders had no role in the design of the study; in the collection, analyses, or interpretation of data; in the writing of the manuscript, and in the decision to publish the results.

## References

1. Adriani, O.; Akaike, Y.; Asano, K.; Asaoka, Y.; Bagliesi, M.G.; Berti, E.; Bigongiari, G.; Binns, W.R.; Bonechi, S.; Bongi, M.; et al. Direct measurement of the cosmic-ray proton spectrum from 50 GeV to 10 TeV with the Calorimetric Electron Telescope on the International Space Station. *Phys. Rev. Lett.* **2019**, *122*, 181102. [CrossRef] [PubMed]
2. An, Q.; Asfandiyarov, R.; Azzarello, P.; Bernardini, P.; Bi, X.J.; Cai, M.S.; Chang, J.; Chen, D.Y.; Chen, H.F.; Chen, J.L.; et al. Measurement of the cosmic-ray proton spectrum from 40 GeV to 100 TeV with the DAMPE satellite. *Sci. Adv.* **2019**, *5*, eaax3793. [PubMed]
3. Alemanno, F.; An, Q.; Azzarello, P.; Barbato, F.C.T.; Bernardini, P.; Bi, X.J.; Cai, M.S.; Catanzani, E.; Chang, J.; Chen, D.Y.; et al. Measurement of the cosmic ray helium energy spectrum from 70 GeV to 80 TeV with the DAMPE space mission. *Phys. Rev. Lett.* **2021**, *126*, 201102. [CrossRef] [PubMed]
4. Zhang, S.N.; Adriani, O.; Consortium, H.; Albergo, S.; Ambrosi, G.; An, Q.; Azzarello, P.; Bai, Y.; Bao, T.; Bernardini, P.; et al. Introduction to the High Energy cosmic-Radiation Detection (HERD) Facility onboard China's FutureSpace Station. *Proc. Sci.* **2017**, *301*, 1077.
5. Atwood, W.B.; Bagagli, R.; Baldini, L.; Bellazzini, R.; Barbiellini, G.; Belli, F.; Borden, T.; Brez, A.; Brigida, M.; Caliandro, G.A.; et al. Design and initial tests of the Tracker-converter of the Gamma-ray Large Area Space Telescope. *Astropart. Phys.* **2007**, *28*, 422–434. [CrossRef]
6. Bulgarelli, A.; Argan, A.; Barbiellini, G.; Basset, M.; Chen, A.; Di Cocco, G.; Foggetta, L.; Gianotti, F.; Giuliani, A.; Longo, F.; et al. The AGILE silicon tracker: Pre-launch and in-flight configuration. *Nucl. Instruments Methods Phys. Res. Sect.* **2010**, *95*, 213–226. [CrossRef]
7. Adriani, O.; Ambrosi, G.; Azzarello, P.; Basti, A.; Berti, E.; Bertucci, B.; Bigongiari, G.; Bonechi, L.; Bongi, M.; Bottai, S.; et al. Tracker-In-Calorimeter (TIC): A calorimetric approach to tracking gamma rays in space experiments. *J. Instrum.* **2020**, *15*, P09034. [CrossRef]
8. Starodubtsev, O.; Adriani, O.; Bongi, M.; Bottai, S.; D'Alessandro, R.; Detti, S.; Lenzi, P.; Mori, N.; Papini, P.; Vannuccini, E.; et al. Development of a homogeneous, isotropic and high dynamic range calorimeter for the study of primary cosmic rays in space experiments. *Proc. Sci.* **2015**, *189*, 1–9. [CrossRef]
9. Adriani, O.; Albergo, S.; Auditore, L.; Basti, A.; Berti, E.; Bigongiari, G.; Bonechi, L.; Bongi, M.; Bonvicini, V.; Bottai, S.; et al. The CaloCube project for a space based cosmic ray experiment: Design, construction, and first performance of a high granularity calorimeter prototype. *J. Instrum.* **2019**, *14*, P11004.
10. Adriani, O.; Bonechi, L.; Bongi, M.; Castellini, G.; Ciaranfi, R.; D'Alessandro, R.; Grandi, M.; Papini, P.; Ricciarini, S.; Tricomi, A.; et al. The construction and testing of the silicon position sensitive modules for the LHCf experiment at CERN. *J. Instrum.* **2010**, *5*, P01012.
11. Battistoni, G.; Boehlen, T.; Cerutti, F.; Chin, P.W.; Esposito, L.S.; Fassò, A.; Ferrari, A.; Lechner, A.; Empl, A.; Mairani, A.; et al. Overview of the FLUKA code. *Ann. Nucl. Energy* **2015**, *82*, 10–18. [CrossRef]
12. Fermi Collaboration, Fermi LAT Performance. Available online: https://www.slac.stanford.edu/exp/glast/groups/canda/lat_Performance.htm (accessed on 19 September 2022). [CrossRef]
13. Chang, J.; Ambrosi, G.; An, Q.; Asfandiyarov, R.; Azzarello, P.; Bernardini, P.; Bertucci, B.; Cai, M.S.; Caragiulo, M.; Chen, D.Y.; et al. The DArk Matter Particle Explorer mission. *Astropart. Phys.* **2017**, *95*, 6–24. [CrossRef]

14. Azzarello, P.; Ambrosi, G.; Asfandiyarov, R.; Bernardini, P.; Bertucci, B.; Bolognini, A.; Cadoux, F.; Caprai, M.; De Mitri, I.; Domenjoz, M.; et al. The DAMPE silicon-tungsten tracker. *Nucl. Instruments Methods Phys. Res. Sect.* **2016**, *831*, 378–384.
15. Ackermann, M.; Ajello, M.; Allafort, A.; Asano, K.; Atwood, W.B.; Baldini, L.; Ballet, J.; Barbiellini, G.; Bastieri, D.; Bechtol, K.; et al. Determination of the Point-Spread Function for the Fermi Large Area Telescope from On-Orbit Data and Limits on Pair Halos of Active Galactic Nuclei. *Astrophys. J.* **2013**, *54*, 765. [CrossRef]